J. H. Schmertmann[1]

Authorized Reprint from
Special Technical Publication 740

1981

A General Time-Related Soil Friction Increase Phenomenon

REFERENCE: Schmertmann, J. H., **"A General Time-Related Soil Friction Increase Phenomenon,"** *Laboratory Shear Strength of Soil, ASTM STP 740*, R. N. Yong and F. C. Townsend, Eds., American Society for Testing and Materials, 1981, pp. 456-484.

ABSTRACT: Various laboratory treatments of clay specimens produced an increase in the frictional component of their ability to mobilize shear resistance. These treatments included compression after isotropic normal consolidation, compression after isotropic overconsolidation, anisotropic normal consolidation, chemically induced dispersion, changing pore fluid, decreasing rate-of-strain, increasing time for secondary compression, and allowing time for creep. The paper shows how increasing clay fabric dispersion in these treatments relates directly to an increased friction capability. The author then suggests that the dispersion shifts the external shear load to stiffer and stronger aggregates of particles in the fabric. This produces a stiffer and stronger clay due to its increased frictional capability. The practical aspects of this behavior include a better understanding of various laboratory specimen aging effects such as increasing modulus and the quasi-preconsolidation effect, recognizing it as a frictional and not a bonding behavior, and the desirability of including such behavior in the laboratory or computer simulation of *in situ* performance.

KEY WORDS: soils, soil tests, shear properties, clays, fabric, compressibility, aging, time effects, friction

Nomenclature

A	Pore pressure parameter $= [\Delta u/\Delta(\sigma_1' - \sigma_3')]$
A_q	Net value of A during quasi-preconsolidation (2-4 ESP in Fig. 12)
c'	Empirical Mohr-Coulomb cohesion intercept in terms of effective stress
c_ϵ	Early notation for I_ϵ
d_ϵ	Alternative expression for the D-component, $= \Delta\tau/\Delta\sigma'$
D	Component of mobilized shear resistance seemingly linearly dependent on effective stress, σ', at constant structure
E	Young's modulus

[1]Principal, Schmertmann and Crapps, Inc., Gainesville, Fla. 32601.

ESP	Effective stress path
G	Shear modulus
G_s	Specific gravity of soil solids
iNC	Isotropically normally consolidated
iOC	Isotropically overconsolidated
I	Component of mobilized shear resistance seemingly independent of effective stress, σ', at constant structure. Note $I + D = \tau$
I_ϵ	Notation for I to emphasize that component is a function of strain, value of I at strain ϵ
IDS-test	Experimental procedure for determining the I and D components of τ as functions of strain. Usually done with ϵ and u control
I_m	Maximum value of I determined from a graph of I versus strain
I_0	Mobilized shear resistance when $\sigma' = 0$, the bond shear resistance
K_0	Ratio of σ_3'/σ_1' during virgin consolidation
NC	Normally consolidated
OC	Overconsolidated
p_c	Preconsolidation pressure
p_0	Normal consolidation pressure
Δp_{cq}	Increment of apparent p_c due to quasi-preconsolidation effect
PI	Atterberg plasticity index
R	Overconsolidation ratio
S_2	Value of $[(1 - K_0)/(1 + K_0)]$ before secondary compression aging
S_4	Value of $[(1 - K_0)/(1 + K_0)]$ at start of new increment of virgin consolidation
u	Pore water pressure
w_L	Atterberg liquid limit
w_p	Atterberg plastic limit
w_s	Atterberg shrinkage limit
X_s	Fraction of β-strength increase mobilized during secondary aging
β	Parameter relating I-component to effective stress [1][2]
Δ	Denotes "an increment of"
ϵ	Strain
σ	Total normal stress
σ'	Effective normal stress, $= \sigma - u$
σ_1'	Major principal effective stress
$\bar{\sigma}_1'$	Average value of σ_1' (bar denotes average value)
σ_3'	Minor principal effective stress
σ_{1h}'	Higher effective stress level in an *IDS*-test
$\sigma_{1\ell}'$	Lower effective stress level in an *IDS*-test
τ	Mobilized shear resistance

[2]The italic numbers in brackets refer to the list of references appended to this paper.

ϕ'	Empirical soil friction strength angle in terms of effective stress
ϕ_ϵ'	Early notation for D-component, $= \tan^{-1} d_\epsilon$
ϕ_m'	Part of ϕ' actually mobilized

The Bjerrum Memorial Volume (BMV) contains a paper by the author [*1*] that presents a detailed summary of laboratory research aimed at contributing towards a better understanding of the frictional and bond components of shear strength behavior in all soils. Parts of Ref *1* describe a seemingly very common and not generally appreciated shear phenomenon in cohesive soils. This paper extracts and organizes these parts from the parent BMV reference so as to focus on the evidence that relates to and describes this phenomenon.

Any conventional Mohr-Coulomb shear strength envelope shows the combined effects of changes in effective stress and the changes in the soil structure or fabric associated with such changes in effective stress. Reference *1* describes some special experimental methods for separating these effects. Extensive use of these methods, as described herein, shows how the mobilized components of shear strength change with changes in fabric, and how the changes in these components *with time* indicate a dispersive change in structure *with time*. This dispersion then leads to a fabric stress transfer behavior which usually produces a stronger and stiffer clay due to increased friction-type strength. This work seems to offer a nonbond explanation for the "aging" effects, such as "quasi-preconsolidation", sometimes observed in lab clay specimens.

Understanding this phenomenon first requires a brief explanation of the special soil shear resistance components used by the author, and the laboratory test method used to determine them.

The d_ϵ-Component and the *IDS*-Test

Geotechnical engineers usually find it convenient to separate the shear strength of soil into components. The most common set of such components results from the linear approximation of the Mohr-Coulomb failure envelope, giving the friction (slope) and cohesion (intercept) components. However, the apparently linear or nearly linear envelope often determined from conventional series of consolidated-undrained or drained shear tests represents only an empirical result for the convenience of engineering analysis. The empiricism results from both the linear approximation and from the fact that the envelope combines the effects of changes in stress and the laboratory changes in soil structure resulting from the changes in stress.

Many investigators, including the author in the BMV, have shown that the Mohr-Coulomb shear strength envelope has significant curvature. This curvature becomes especially apparent when the investigator determines the

envelope from a series of shear tests designed to maintain the structure of the soil as nearly constant as possible while testing over the required range of effective stress [*1*]. Consider the general case of a curved envelope as shown by *x-y-z* in Fig. 1. This figure also illustrates one way of representing the shear strength of any point *y* on the envelope by means of the sum of the two components labeled *I* and *D* in the figure. The first step to obtain these components at point *y* requires constructing a tangent to the curve at that point. This tangent then intercepts the $\sigma' = 0$ axis at point *c*. Thus we can say that the illustrated soil behaves at point *y* as if it had an effective stress independent component of *I* and an effective stress dependent component of *D*. The ratio of $(D/\sigma')_y$ denotes the shear strength sensitivity of the soil at point *y* to varying the effective stress. It thus gives a point value of fabric friction capability. The author has given this ratio the symbol d_ϵ as shown in Eq 1. The ϵ-subscript emphasizes that the mobilization of *d* depends on strain.

$$d_\epsilon = \frac{D}{\sigma'} = \frac{\Delta\tau}{\Delta\sigma'} \tag{1}$$

Note that the intercept *I*-component does not represent the correct value of $\sigma' = 0$ intercept strength that the Fig. 1 soil could actually mobilize. I_0 and not *c* represents the correct intercept strength. For ordinary envelope curvatures for clay the value of *I* can considerably exceed the value of I_0. In fact, Ref *1* shows that noncemented clays often have negligible values of I_0. Thus *I* does not designate a physical cohesion or bond strength for the soil illustrated in Fig. 1. Instead it represents an intercept obtained by extrapolating a tangent to the envelope curve. The BMV paper shows that the *I*-component has a surprisingly constant and unique behavior that appears related to the radii of the edges of the particles in contact and therefore to a

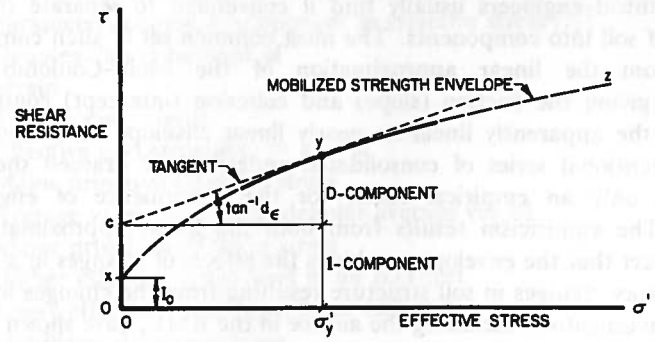

FIG. 1—*Curved Mohr constant-structure envelope showing the definition of the* I- *and* D-*components of mobilized shear strength.*

soil's grain size and mineralogical distribution. This aspect of *I*-behavior falls beyond the scope of this paper. However, this paper will subsequently show some of the uniqueness of the *I*-component in conjunction with discussions of d_ϵ-behavior.

While the profession normally uses the Mohr-Coulomb envelope for a defined failure condition, such as maximum shear or maximum stress ratio, in principle one can construct such an envelope for any defined mobilized shear strength condition such as that mobilized at a given value of test sample strain. Other envelopes could represent the mobilized strength at other values of strain. The investigator could then plot the variation of the *I* and *D* strength components as functions of strain at any constant magnitude of effective stress, such as σ_y' in Fig. 1.

The author has accomplished the separation of the *I* and *D* components as functions of *S*train by means of a laboratory testing procedure appropriately designated the *IDS*-test. The BMV reference [*1*] describes this test in detail, as do Schmertmann and Osterberg [*2*] and Schmertmann [*3,4*]. Briefly, the test consists of subjecting a soil to a nondestructive change in effective stress conditions cycled between two constant reference states, such as two constant values of σ_1', which the investigator maintains constant by appropriate control of pore pressure over the complete strain range of the test. By interpolation the investigator obtains two complete stress-strain curves, one for each effective stress level. From these he or she can show how the *I* and *D* components varied with strain. The previous references give many examples of the results from this type of testing. By this method one can determine the effective stress sensitivity of the mobilized shear strength, the value of d_ϵ in Eq 1, as a function of strain simply by dividing the *D*-component at each strain by the current average value of effective stress.

Soil Treatments that Produce an Increase in d_ϵ

As part of his shear strength research the author subjected soil samples to a variety of stress, chemical, and time-related treatments, and studied their effects on the strain mobilization of the *I* and *D* components of shear resistance. Many of these treatments produced important changes in maximum shear resistance or the strain rate of mobilization of resistance, or both. But, to the author's great surprise at the time, the *I*-component remained constant during most of these treatments. The changes in mobilized shear resistance behavior resulted almost entirely from changes in the *D*-component and therefore in d_ϵ. This section discusses the various treatments and their effects on these strength components and on fabric dispersion. This section will also make use of the term "dispersion" with the soil fabric or soil structure meaning first suggested by Lambe [*5*].

Fabric Dispersion

The initial formation and structure of clays with their platy-shaped particles, or aggregates of such particles, involves many edge-to-face or edge-to-edge contacts. Lambe [5] referred to clays with a large proportion of such contacts as having a "flocculent" fabric or structure, which tends to produce a random orientation of particles. Distortions or other modifications of this structure which reduce the number of such contacts tend to produce a more oriented and parallel arrangement between the clay particles or aggregates of such particles. Lambe referred to this type of fabric or structure modification as "dispersion". When a clay reaches the state of having a predominantly parallel fabric, he referred to it as "dispersed". The following eight sections will show that mobilizing d_ϵ appears to correlate with dispersion.

Note that dispersion under undrained conditions tends to decrease stiffness and strength, as usually happens when remolding an undisturbed clay at constant water content. However, dispersion with drainage may have an entirely different effect. A typical *IDS*-test cycles between two constant-σ_1' conditions and allows whatever drainage required to maintain σ_1' constant during the strain.

Compression of isotropically, Normally Consolidated (iNC) Clay

At the very beginning of the research in developing and using the *IDS*-test [2] the author discovered that after the typical, one-day, isotropic, normal consolidation a clay would fully mobilize its *I*-component at 1 percent or less axial strain but only gradually mobilize its *D*-component. Figure 2 and the solid lines in the lower half of Figs. 3 and 4 illustrate such test results from two clays. Table 1 lists some of the mineralogical properties of these and the other clays involved in this paper. Note the very rapid rise, probably essentially elastic, in the *I*-component compared with the much more gradual development of d_ϵ. It appears that mobilizing d_ϵ requires significant axial strain. This strain implies significant shear strain and significant movement between soil particles.

We know that shear strain tends to disperse structure. In the extreme of the very high strain, residual state, we have a high degree of dispersion in the planes of shear movement. We thus have the first connection between d_ϵ and dispersion—both increase with strain. The final, 10 percent strain components in Fig. 2 reinforce this connection. At a strain between 6 and 10 percent this sample developed a distinct shear plane, which produced an otherwise unusual abrupt drop in *I* and a corresponding increase in *D* and d_ϵ. We associate the shear plane and its high shear strains with locally increased soil structure dispersion, and thus have this test to connect more directly an increasing d_ϵ with increasing dispersion. See Ref 2, p. 665, for more details about this test.

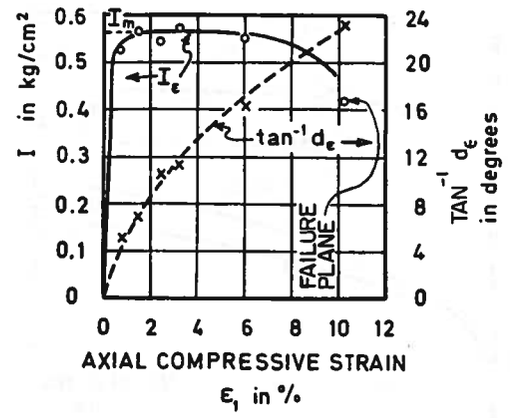

FIG. 2—*Example of the determination of the* I *and* D *components as functions of strain (1 kg/cm² = 98 kPa = 1.02 tsf).*

Compression After One Cycle of isotropic Overconsolidation (iOC)

Figures 3 and 4 also show the stress-strain curves (top half of figure) and the component mobilization curves (bottom half of figure) after one-cycle overconsolidation by ratios of 4 and 3, respectively. Note that this overconsolidation produces a large increase in shear strength, greatest at low strain and diminishing with additional strain. Note also that this increase occurs while maintaining effective stress levels approximately the same as those used in the similar *IDS*-test on the comparative iNC sample. The component curves show that essentially the entire strength increase from overconsolidation results from a large increase in d_ϵ. The strain mobilization of the *I*-component remains essentially the same as for the iNC clay.

The process of overconsolidation not only increases the density of particle packing but on the micro-fabric level the densification process reduces void space and therefore must force the platy particles into a more parallel orientation. Overconsolidation tends to disperse structure. We thus have further evidence that dispersion has the net effect of increasing d_ϵ.

Anisotropic Consolidation

Schmertmann and Hall [6] investigated the effect of anisotropic consolidation at various $K' = \sigma_1'/\sigma_3'$, ratios but using the same σ_1' magnitude at each K'. Figure 5 shows some of the results from their comparative testing. They found that the subsequent compressive strength of both kaolinite and Boston blue clay increased as the normal consolidation K'-ratio increased. This occurred despite the reduced consolidation σ_3' magnitude as K' in-

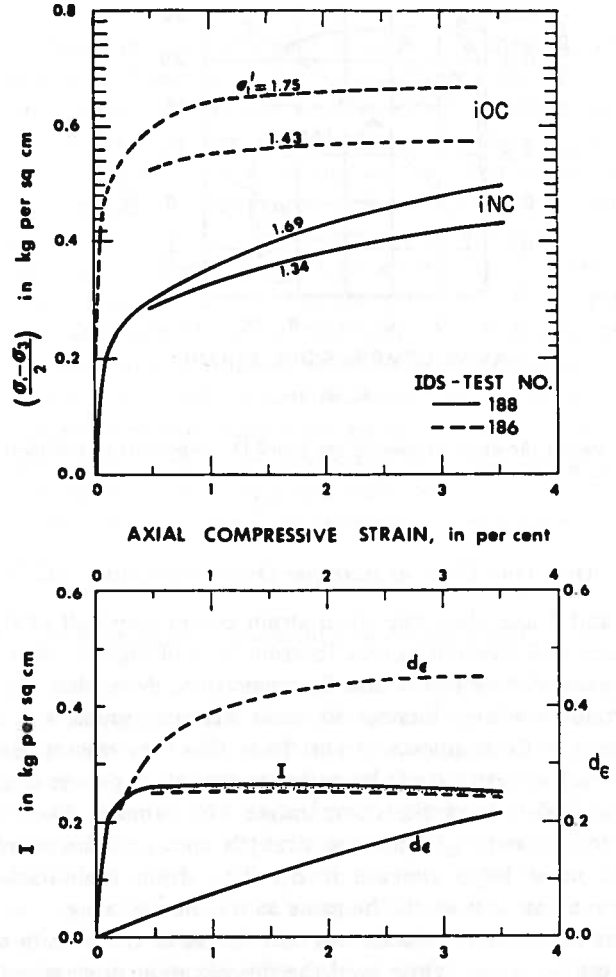

FIG. 3—*Comparisons of shear component mobilization in NC and OC* (R = 4) *extruded Enid clay (1 kg/cm² = 98 kPa = 1.02 tsf).*

creased. Note that once again the after-consolidation compressive strain mobilization of the *I*-component did not change. The strength mobilization increases due to anisotropic consolidation appeared due entirely to increases in the *D*-component. These increases gradually reduced with increasing compressive strain, but they still had a significant magnitude at 5 percent compressive strain in the *IDS*-test that followed the *K'*-consolidation.

Increasing the *K'*-ratio during normal consolidation produced successively increased vertical strain during that consolidation. As discussed in the section on Compression of iNC Clay, more strain might mean more dispersion and therefore help explain the greater d_ϵ at the beginning of the compression test that followed the consolidation.

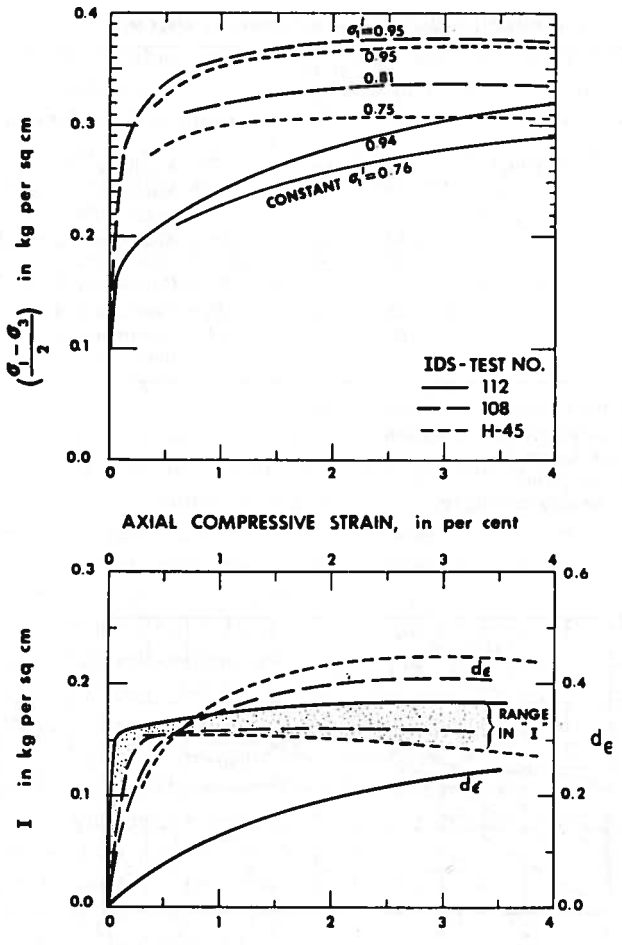

FIG. 4—*Comparisons of shear component mobilization in NC and OC* (R = 3) *extruded kaolinite clay (1 kg/cm² = 98 kPa = 1.02 tsf).*

Chemically Induced Dispersion

The addition of small amounts of chemicals to a cohesive soil can sometimes cause dramatic changes in its fabric. The author added sodium phosphate dispersants to kaolinite and Boston blue clays (BBC) before machine remolding and extruding some of the triaxial test specimens. These dispersants had the effect of reducing the shrinkage limit and plasticity index

TABLE 1—*Plasticity and mineralogy of clays tested.*

Remolded Clay	PI, %	0.002 mm. %	Activity	Clay Minerals
Dispersed kaolinite (Q-EPK)	4	60	0.07	Kaolinite—99%
Enid (residual)	9	20	0.45	Kaolinite—15% Illite—10%
Jacksonville	14	13	1.08	Montmorillonite—10%
Boston blue	19	53	0.36	Illite—45% Chlorite—25%
Kaolinite	21	60	0.35	Kaolinite—99%
Lake Wauberg	105	85	1.24	Montmorillonite—85% Illite—5%

All I_m results from constant-σ_1' *IDS*-tests using:
isotropic consolidation to 3.50 kg/cm^2,
$\sigma_{1\,high}' = 3.30$ kg/cm^2,
$\sigma_{1\,low}' = 2.60$ kg/cm^2,
1 kg/cm^2 = 98 kPa = 1.02 tsf.

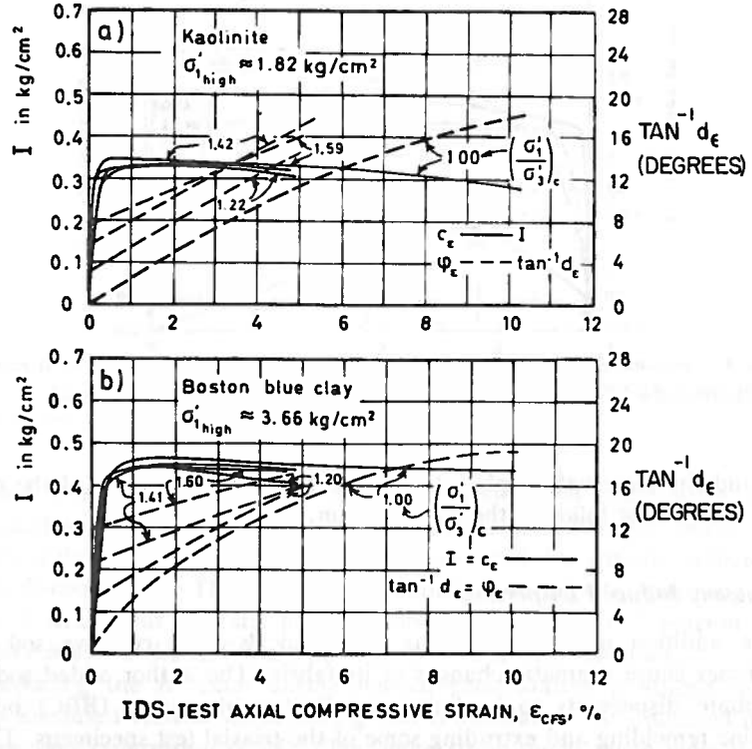

FIG. 5—*Strain mobilization of the* I *and* D *components after about 20-h anisotropic secondary consolidation (1 kg/cm^2 = 98 kPa = 1.02 tsf)* [6].

of each clay, and progressively reducing the equilibrium void ratio at a given effective stress (Table 2*a*). These progressive effects followed from the presumed progressive increase in clay fabric dispersion resulting from adding a more powerful dispersant chemical.

Table 2*a* also shows that such progressive dispersion had essentially no effect on the maximum value of the *I*-component, I_m. In contrast, Table 2*b* lists a dramatic increase in d_ϵ at the selected representative compressive strains of 1 and 3 percent. This appears to offer direct evidence of the unique connection between increased clay fabric dispersion and increased d_ϵ—at least at low relative (to residual state) shear strain.

Changing a Clay's Pore Fluid

Starting with a still hot, oven-dried kaolinite powder, the author prepared dry triaxial test specimens and then vacuum-saturated them with five different pore fluids ranging in viscosity from dry nitrogen to a 25 percent glycerine and 75 percent water mixture. Table 3 lists information about these samples. After near-saturation of the kaolinite with these various fluids, the author performed an ordinary *IDS*-test of the constant-σ_1' type, using the same effective stress levels for all the comparative tests. Figure 6 shows the comparative strength component results as a function of strain. Once again, the *I*-component behavior seems about the same for all the tests. Also once again, the d_ϵ-values show dramatic differences. The less the viscosity of the pore fluid, the greater the value of d_ϵ mobilized at a given strain.

It appears that for the same rate-of-strain conditions in this series of comparative tests that more movement between particles can take place within a given time or strain interval as the pore fluid viscosity decreases. This seems reasonable because the lower the viscosity the more easily the pore fluid can move out of the way and not retard the particle movements. One can also explain this by saying that a lower viscosity allows more dispersion per unit strain and therefore a more rapid mobilization of d_ϵ.

Note that the increase in d_ϵ with decreasing viscosity took place despite a large increase in test void ratio with this decreased viscosity. Such a void ratio increase by itself should reduce particle inference effects and therefore reduce d_ϵ. It appears that an even larger viscosity effect dominated the combined behavior.

Decreasing Rate of Strain

In their closure in 1962 Schmertmann and Hall [7] presented the results from a series of *IDS*-tests on duplicate specimens of extruded kaolinite in which all variables remained constant except rate-of-strain. This rate varied by a factor of over 5000 for the seven tests involved in this comparative series. Figure 7, copied from this discussion, shows the comparative high-σ_1' stress-

TABLE 2a—*Effects of chemical dispersion on plasticity, void ratio, and mobilized shear strength components:* I_m *versus structure at* $\bar{\sigma}_f' = 2.95$ kg/cm^2 (1 kg/cm^2 = 98 kPa = 1.02 tsf).

Clay	Abbreviation	Shrinkage Limit (SL)	PI	Void Ratio	I_m, kg/cm^2	Structural Condition
Kaolinite	DWEPK	25.0	21	0.888	0.54	Extruded, no chemical dispersion
Kaolinite	N-EPK	21.9	8	0.783	0.50	$Na_2HPO_4 7H_2O$ dispersed
Kaolinite	DWEPK	...	21	0.898	0.57	Extruded, no chemical dispersion
Kaolinite	Q-EPK	19.2	4	0.674	0.56	$Na_6P_4O_{13}$ dispersed
Boston Blue clay	BBC	...	19	0.659	0.50	Extruded, no chemical dispersion
Boston Blue clay	BBC	...	19	0.648	0.46	Extruded, no chemical dispersion
Boston Blud clay	Q-BBC	...	11	0.532	0.49	$Na_6P_4O_{13}$ dispersed

TABLE 2b—*Effects of chemical dispersion on plasticity, void ratio, and mobilized shear strength components: Examples of pre-dispersion of soil structure increasing strain-rate of* d_ϵ*-mobilization.*

Extruded Soil	Average $\tan^{-1} d_\epsilon$ (deg) at *IDS*-Test Axial Compressive $\epsilon_1 = 1.0\%$	$\epsilon_1 = 3.0\%$
Kaolinite (DW-EPK)	3.5	9
N*-EPK	5	11
Q*-EPK	10	19
Boston blue clay (BBC)	4	10
Q*-BBC	8	16

*Denotes addition of sodium phosphate dispersant prior to extrusion.

strain curves and also the comparative I and D components of mobilized shear resistance.

Once again, the I-component remains approximately constant. But the strain-mobilization of d_ϵ increases significantly with decreasing rate-of-strain. It appears that reducing the rate-of-strain allows the soil particles more time to interact with each other and therefore to develop a higher value of d_ϵ at a given strain. This would also follow from the previous concept of decreasing viscosity allowing greater soil structure dispersion. Increasing the time at a constant pore fluid viscosity should have the same effect as decreasing viscosity while time remains constant.

These data now begin to show how increasing time produces a larger d_ϵ-component. Other examples now follow.

Increasing Time for Secondary Compression

A series of tests in which the author allowed progressively increasing times for secondary compression (under constant effective stress conditions) proved informative. Figure 8 shows the *IDS*-test components obtained from this comparative series, again on remolded kaolinite, with all other test conditions the same. Note again that I_m remains about the same with any differences probably due mostly to experimental variations. Again, in contrast, there occurs a dramatic increase in the rate of d_ϵ-mobilization with strain, especially at low strains. This dramatic increase occurred despite the fact that this kaolinite had a typical very low coefficient of secondary compression. The effect of time seems most pronounced at the beginning strains of the *IDS* compression tests following the secondary consolidation. It decreases with additional strain and appears destroyed in this soil after about 3 percent compressive strain.

The heavy line in Fig. 8 shows, again for comparative purposes, the *IDS*-test d_ϵ-component from the same kaolinite clay, but deliberately dispersed

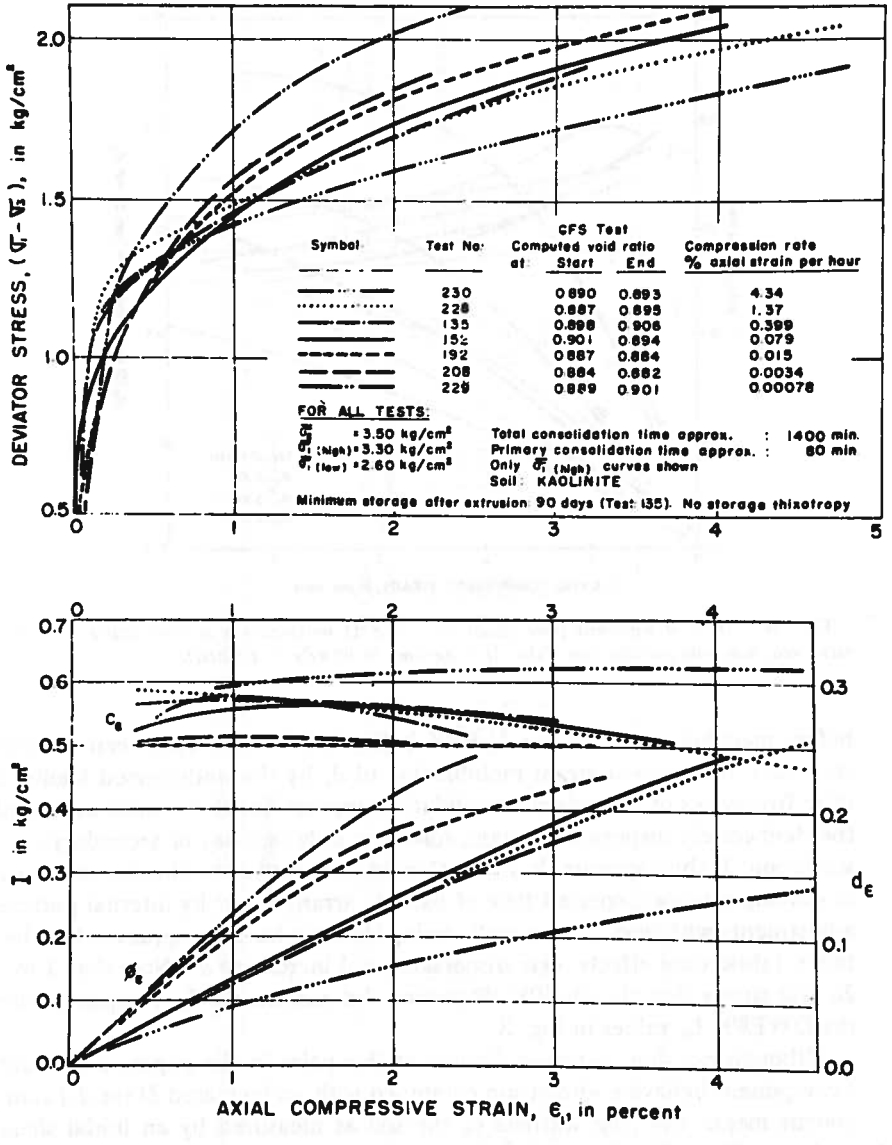

FIG. 7—*Effect of rate of compressive strain on the* IDS*-test results obtained from duplicate specimens of remolded, saturated kaolinite clay (1 kg/cm² = 98 kPa = 1.02 tsf).*

specialty have also recognized the clay structure stiffening effect from secondary consolidation. For example, see Anderson and Woods [*9*]. This fact has introduced the need for a correction factor of about 1.5 to 3.5 before using lab-determined *G*-values for the *in situ* clay.

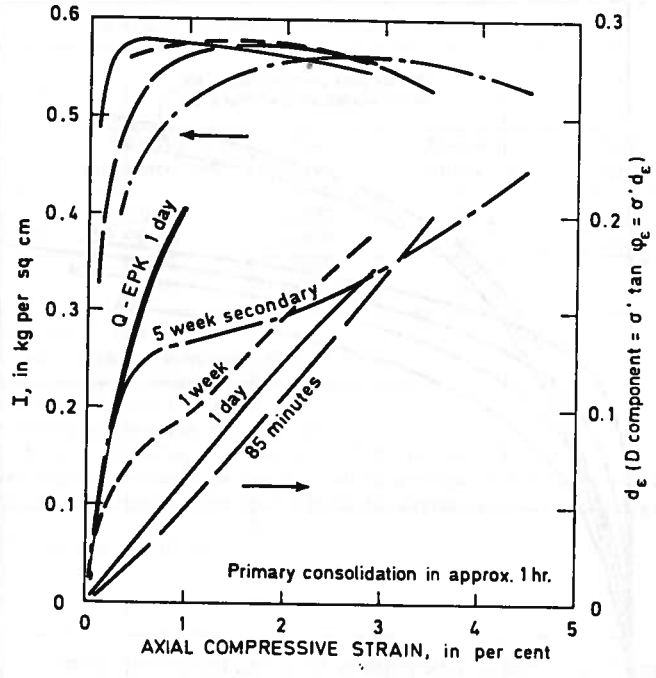

FIG. 8—*Effect of secondary isotropic consolidation times on* I *and* D *in extruded kaolinite clay (1 kg/cm² = 98 kPa = 1.02 tsf).*

These results suggest that small differences in clay fabric can have large consequences. They also suggest an explanation for the quasi-preconsolidation effect. Figure 8 shows that the stiffening of the structure with increasing secondary time results from the low-strain increase in d_ϵ. Figures 3 and 4 and the discussion in the section on Compression after One Cycle of Isotropic Overconsolidation show the same increase in d_ϵ with overconsolidation. Hence for a small increment of additional strain following secondary consolidation the clay will behave as an overconsolidated clay. A later section of this paper quantitatively discusses the quasi-preconsolidation effect.

Time for Undrained Creep

Bea [*10*] performed a series of undrained creep tests following isotropic, normal consolidation of both kaolinite and remolded and undisturbed samples of Boston blue clay. These samples strained slowly with time under a constant axial compressive deviator stress. After such creep he performed *IDS*-tests in which he forced a controlled strain rate upon the clay greater than the prior creep strain rate. He used the *IDS*-tests to separate the components of mobilized shear strength over the additional *IDS*-test strains,

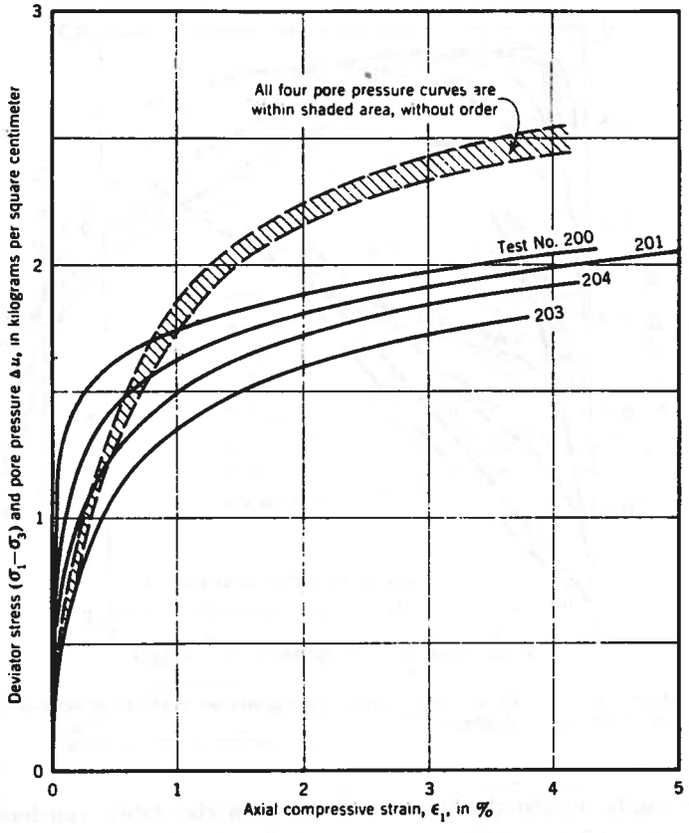

FIG. 9—*Example of secondary shear strength behavior: consolidated-undrained compression of machine extruded and saturated kaolinite (1 kg/cm² = 98 kPa = 1.02 tsf).*

and, by back-extrapolation, also at the end of creep. He then compared these results with the component separations from duplicate specimens not subjected to such creep. Figure 10 presents some of his results from kaolinite, and Fig. 11 and Table 5 from Boston blue clay. The explanations now given should help the reader to understand the unavoidably complex Figs. 10 and 11.

Figure 10 first shows the no-prior-creep reference *I*- and *D*-component strain mobilization curves from replicate tests H-13 and B-1. These tests produced mobilization curves that almost coincide—the solid lines for *I* and the dashed lines for *D*. Bea then superposed the component mobilization results from *IDS*-tests performed after allowing three samples of the same clay to undergo different values of compressive strain during creep under constant deviator stress. Creep test No. 2 had a constant deviator stress of 1.12 kg/cm²

TABLE 4—*Details of comparative tests shown in Fig. 9.*

Test No.	Time in Secondary, min	Computed: Void Ratio	Computed: Degree of Saturation	Initial Tangent Modulus, E_i, kg/cm²/Σ_1 %
200	35600	0.882	99.5	90
201	9920	0.879	99.8	insufficient data
204	1310	0.880	99.7	35
203	115	0.883	100.0	9

Initial void ratio = 1.013.
Isotropic consolidation, 1-increment, 0 to 3.5 kg/cm²
End of primary (Casa. construction) = 85 min.
Strain rate approximately 1 % in 6 h.
Constant triaxial cell pressure = 3.5 kg/cm².
G_s = 2.609, w_L = 52 %, w_p = 31 %, w_s = 25 %, 60 %—2 microns.
The initial tangent modulus is the average modulus between the first and third data points obtained during the compression (after the 0-0 point; the deviator stress at these points was 0.1 and 0.5 kg/cm².
1 kg/cm² = 98 kPa = 1.02 tsf.

for 9 days,[3] which produced an axial compressive strain of 0.7 percent. The subsequent *IDS*-test obtained the *I*-component data shown by the solid square points and the *D*-component data shown by the + symbols. Comparison with the reference mobilization curves shows almost no change in *I*-component mobilization, but does show the large increase in *D*-component mobilization illustrated by the cross hatching beginning at 0.7 percent strain.

Similarly in Fig 10, creep test No. 3 under the greater deviator stress of 1.68 kg/cm² produced 1.7 percent axial strain during 10 days of creep. The subsequent *IDS*-test produced the solid triangles for the *I*-component determinations and the open circles for the *D*-component determinations. One can again see almost no change in *I*-component mobilization as a result of the prior creep, but can easily see the large increase in *D*-component mobilization illustrated by the different cross hatching beginning at 1.7 percent strain.

Again in Fig. 10, creep test No. 4 under the still greater constant 1.96 kg/cm² deviator stress produced a strain of 5.0 percent during 11 days of creep. The subsequent *IDS*-test produced the *I*-component determinations shown by the solid circles and the *D*-component determinations shown by the x symbol. One can again see only minor change in *I*-component mobilization as a result of the prior creep, but can easily see the increase in *D*-component mobilization illustrated by the cross hatching beginning at 5.0 percent strain.

The reader will see that for the first 1 to 2 percent of additional and forced

[3] 1 kg/cm² = 98 kPa = 1.02 tsf.

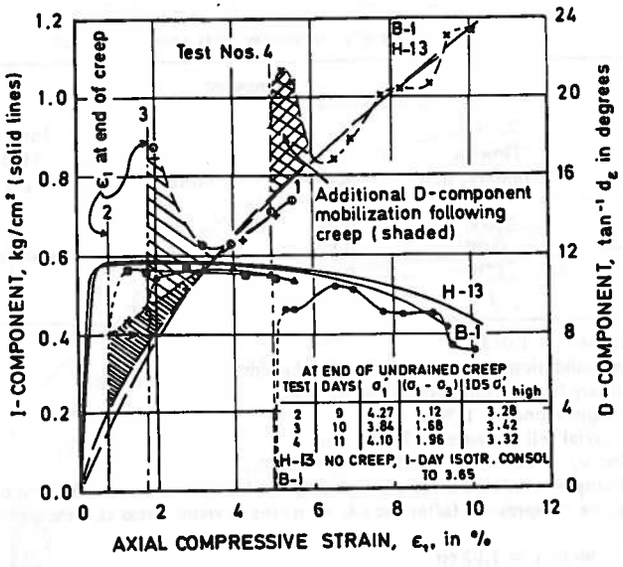

FIG. 10—*Effect of undrained creep on shear component mobilization in remolded kaolinite (1 kg/cm² = 98 kPa = 1.02 tsf)* [10].

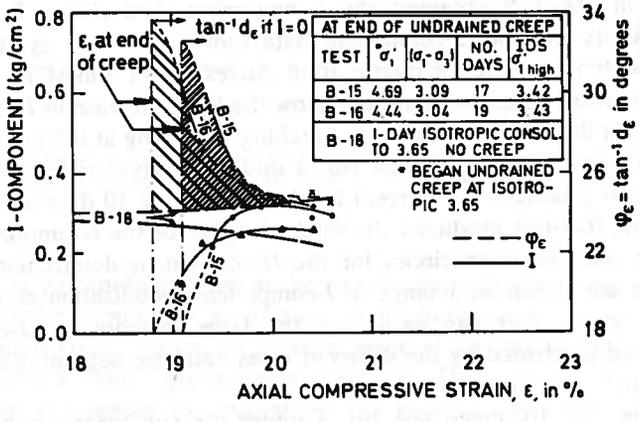

FIG. 11—*Example of excess D-component mobilization after undrained creep in remolded Boston blue clay (1 kg/cm² = 98 kPa = 1.02 tsf)* [10].

strain following the creep, forced at a constant rate, this machine-extruded kaolinite clay considerably increased its d_ϵ-mobilization compared with the same clay without prior creep. Also note that after only a very small *IDS*-test strain the value of the *I*-component becomes equal to that for the same clay but without the prior creep.

TABLE 5—*Effect of creep on the* I *and* D *components in undisturbed BBC (stresses in kg/cm²).*[a]

	Creep		At End of Creep			Without Creep	
Test	$(\sigma_1 - \sigma_3)$	Days	ϵ_1, %	$\tan^{-1} d_\epsilon$	I	$\tan^{-1} d_\epsilon$	I
B-13	2.02	11	2.50	15.0 deg	0.31	11.0 deg	0.51
B-14	2.00	3	2.00	15.1 deg	0.27	9.5 deg	0.54

[a] 1 kg/cm² = 98 kPa = 1.02 tsf.

Figure 11 shows the same type of behavior noted for the Fig. 10 kaolinite, but this time after creep-straining the remolded Boston blue clay to the comparatively high value of about 19 percent axial strain. Test B-18 data provide the no-creep reference for comparison to the with-creep tests B-15 and B-16. Again, the cross hatching beginning at the strain at the end of creep shows the large increase in mobilized *D*-component following the creep. In this case the $\tan^{-1} d_\epsilon$-component increased about 8 deg as a result of the soil structure adjustments that took place during the 17 to 19 day creep. Table 5 shows that a similar dramatic increase in the *D*-component occurred after subjecting two *undisturbed* samples of Boston blue clay to creep.

The similarity between the changes in the strain mobilization of the *D*-component due to secondary consolidation and due to undrained creep suggests a similar cause. The section on Increasing Time for Secondary Compression suggested clay fabric dispersion as the cause for secondary consolidation. It therefore appears plausible that such dispersion also produces the creep effects discussed in this section.

Hypothesis for Dispersion Producing Increased Friction Resistance

Summary of Dispersion-d_ϵ *Behavior*

A simple forced strain, or simple isotropic consolidation, or anisotropic consolidation with increasing stress ratios, or changing a clay's pore fluid in the direction of reduced viscosity, or inducing prior dispersion by chemical additives: each produced the similar effects of increasing a cohesive soil's subsequent shear resistance sensitivity to a change in effective stress (increasing d_ϵ). These common effects suggest a common cause. In each case the cause seems related to soil fabric dispersion.

Decreasing the rate of strain in a strain-controlled compression test, or increasing the time for one-dimensional secondary consolidation, or increasing the time for anisotropic stress creep behavior also have the common effect of increasing a soil's subsequent d_ϵ-component of strength, but sometimes for only a very limited strain interval in the subsequent forced increased rate of

strain *IDS* compression test. These similar time-related behaviors also suggest a common cause. It seemed possible, for each case, to relate the cause to soil fabric dispersion.

Hypothesis for Dispersion-d_ϵ *Behavior*

The multitude of treatments discussed previously all produce essentially the same effect in terms of the *I* and *D* strength components, thus strongly suggesting that this behavior involves something fundamental in soil fabric response. The author hypothesizes the following behavior: A clay can and will slowly readjust its fabric under drained conditions, such as during long periods of time at constant stress. The more easily dispersed (moved) particles or aggregates of particles yield by particle-to-particle slippages to those particles or aggregates of particles with more rigidity and which probably also have more strength and more resistance to dispersion. Such slippage and consequent yielding produces secondary compression in one-dimensional or isotropic consolidation, or creep if the soil can develop shear strain. With time the soil becomes stronger and stiffer as a result of the yield-transfer of applied shear to those stiffer and stronger aggregates. This transfer shows up as a decrease in the rate of volume change or creep movement. These stronger particle aggregates now find themselves closer to failure, with a greater mobilization of particle friction and interference effects. These effects depend primarily on the magnitude of effective stress. Thus, with the increased strength and stiffness resulting from the load transfer necessitated by dispersive particle movements, we also get an increase in the shear sensitivity of the soil to changes in effective stress, and d_ϵ increases.

A new increment of strain will accompany each subsequent full mobilization of the increased shear resistance capability of the new, more dispersed fabric. When achieving this mobilization in an *IDS*-test the forced strain of the test does not permit the re-occurrence of the dispersive behavior that caused the strengthening to occur. Instead the particle load transfer and strengthening effects that resulted from fabric dispersion break down with the newly forced strain, and the mobilized shear resistance behavior returns to that which would have occurred had the time interval with constant stress and drained dispersion not happened; the data in Figs. 10 and 11 provide examples.

Dispersion-d_ϵ *Phenomenon Affects All Soils*

The data and discussions in this paper have included only cohesive soils because of the more dramatic effects associated with their more complicated fabric and to limit the length of this paper. However, study of Ref *1* will show that the phenomenon probably occurs in all soils. For example, we tacitly admit the existence of a quasi-preconsolidation effect (see the section on Increasing Time for Secondary Compression and the following section) in sands when we use the common assumption of neglecting settlement when the vertical stress increase becomes less than 10 percent of the *in situ* vertical stress.

A Practical Application—The Quasi-Preconsolidation Effect

Leonards and Altschaeffl [*11*] documented in 1964 that after allowing much longer than customary secondary compression aging times following primary consolidation in the laboratory, an otherwise normally consolidated clay behaved as if it had a preconsolidation stress, p_c, greater than the normal consolidation pressure, p_0. They denoted the difference $(p_c - p_0) = \Delta p_{cq}$ as the quasi-preconsolidation effect, and reported that all the clays they tested to that time had shown this effect, with an average ratio of $\Delta p_{cq}/p_0 = 0.40$.

A 40 percent overconsolidation can sometimes have a very important practical value. For example, it might reduce footing settlements to acceptable values and eliminate the need for piles. But many engineers still remain uncertain about the cause and magnitude of this quasi-preconsolidation effect. This section does not present a complete discussion of the subject. Rather, it should show the reader one possibility for a physical and quantitative explanation of the quasi-preconsolidation effect based on the shear strength research results discussed in this paper.

The section on Increasing Time for Secondary Compression has already discussed a possible, perhaps even a probable, cause for this effect involving the similar increase-in-d_ϵ behavior from secondary compression aging and overconsolidation. The author will now attempt a quantitative analysis to determine the magnitude Δp_{cq}, using the experimental results presented herein and in the parent reference [*1*]. Please refer to Fig. 12 to aid this analysis. The effective stress path (ESP) 1-2 shows a clay undergoing an increment of normal consolidation along the appropriate K_0-line, reaching the vertical principle stress consolidation pressure of p_{02}. The clay then ages in secondary compression and increases in strength due to the increase-in-d_ϵ behavior detailed in this paper. By the time the clay again experiences primary consolidation due to an increment of external loading it will have increased its frictional shear strength. But the well-known formula $K_0 \simeq 1 - \sin \phi$; suggests that any increase in ϕ will reduce K_0. Assuming the formula applies, then the next increment of consolidation will begin along some new K_0-line as shown in Figs. 12*a* and 12*b*.

The ESP of the clay must somehow move from Point 2 to a point on the new K_0-line. It may begin this move during the volume change associated with the secondary compression aging under a constant p_{02} effective stress condition. Figure 12*b* illustrates this change. Figure 12*a* shows various constant-*A* ESPs radiating from point 2, where $A = \Delta u/\Delta(\sigma_1' - \sigma_3')$ as usual.

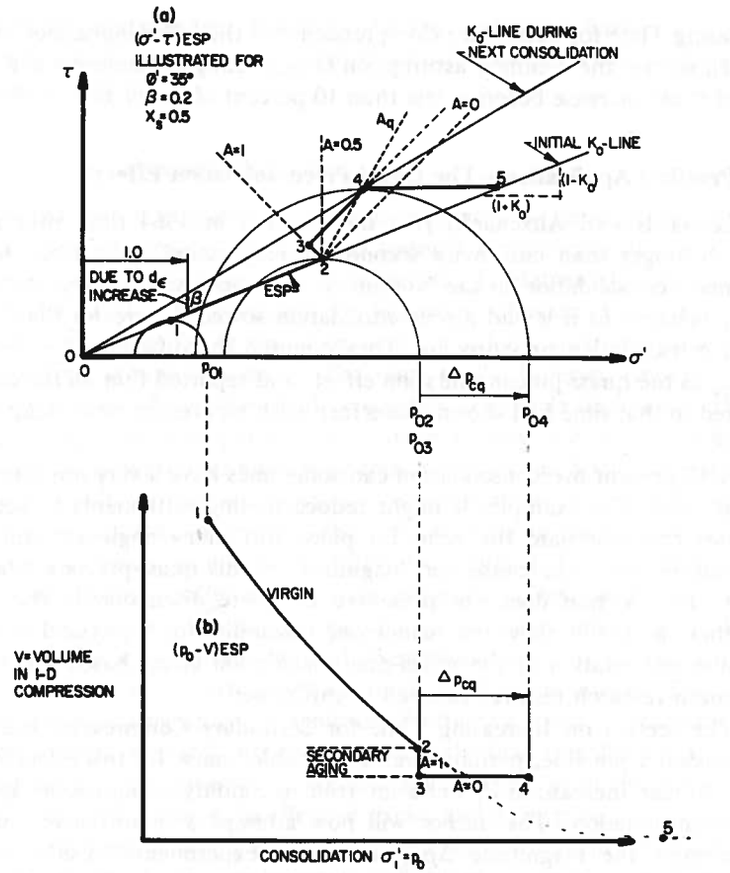

FIG. 12—*Effective stress paths before, during, and after the quasi-preconsolidation process.*

Because of the constant p_{02}, the clay ESP must follow an $A = +1$ or -1 path until it reaches point 3 (illustrated for $A = +1$) at the end of secondary compression aging. After this aging we subject the clay to an increase in σ_1, which tests for the quasi-preconsolidation effect. This effect reaches its maximum when the ESP reaches point 4. After reaching point 4, the additional volume and shear strains associated with further increasing effective stresses gradually destroy the special fabric dispersion effects that increased ϕ' during the 2-3 aging, and the ESP eventually returns to the initial K_0-line at some point 5. Figure 12*a* arbitrarily shows the 4-5 ESP as horizontal (constant τ). Figure 12*b* shows the 4-5 ESP as returning at point 5 to the virgin compression curve applicable to the initial K_0-line because the fabric has now completely lost the special fabric friction-increase effects from the 2-3 aging.

To simplify this discussion, let us imagine the ESP from 3-4 as occurring along another constant-A path. The 3-4 part of the ESP will likely produce little or no volume change. If this path produced no volume change, then the pore pressures generated in a triaxial compression test would equal zero, which in turn would mean that $A = 0$ from 3-4. Figure 12*a* illustrates an assumed $A = 0$, and $\sigma_3' = \text{constant}$, path from 3 to 4 for the actual one-dimensional compression test. Figure 12*b* illustrates the no volume change.

The clay at Point 4 will now have an equivalent consolidation pressure of p_{04}, which, as Fig. 12 shows, may considerably exceed the previous p_{02} and p_{03}. The difference $(p_{04} - p_{02})$ represents the quasi-preconsolidation effect Δp_{cq}. The author has derived a formula for the Δp_{cq} increase ratio from the geometry in Fig. 12*a*. After denoting the $[(1 - K_0)/(1 + K_0)]$ slopes of the K_0-lines as S_2 for the before-secondary aging condition and as S_4 for the after-secondary aging, he then obtained Eq 2:

$$\frac{\Delta p_{cq}}{p_0} = \frac{2(1 - A_q)(S_4 - S_2)}{[1 - (1 - 2A_q)S_4](1 + S_2)} \tag{2}$$

where A_q = the net effect value of A over the entire 2-4 ESP of the quasi-preconsolidation process.

The author next developed an expression for A_q for substitution into Eq 2, using a new term X_s, which denotes the fraction of the 2-4 ESP increase in strength mobilization that occurs during the 2-3 ESP, $A = +1$ or -1, time in secondary compression. Use a negative X_s for a 2-3 ESP along an $A = -1$ path. The remaining fraction of mobilized strength increase then occurs during the assumed 3-4 ESP, $A = 0$, quasi-preconsolidation interval of stress increase. To accomplish the expression for A_q also required the assumption that the conventional $c' = 0$. In addition the writer needed an alternative expression for the increase in mobilized strength, expressed to this point as $(S_4 - S_2)$. As shown in Figs. 5, 10, and 11, and as detailed further in Reference *1*, during times of rest at constant stress the fabric dispersion causes the I-component of applied and mobilized shear to reduce to near-0 with a matching increase in the D-component to still carry the applied shear. Subsequent forced strain then remobilizes the same I-component with very little additional strain, while the increased D-component still remains effective for a longer interval of additional strain. Thus the total mobilized shear resistance of the clay increases by the magnitude of the I-component for a small interval of strain at increased strain rate following a time interval of aging or creep strain rate. However, the increased shear resistance occurs as an increase in d_ϵ. Reference *1* demonstrates that the value of the I-component in

a clay depends primarily on the magnitude of effective stress, with a proportionality constant denoted β. Thus, the tan ϕ_m' along S_2 can increase by β along S_4. Making use of all the above, plus the geometry shown in Fig. 12*a*, allowed the derivation (after much manipulation) of the Eq 3 expression for A_q.

$$A_q = \frac{1}{2}\left\{1 - \left[\frac{(1 - 2X_s) + (S_2 + \beta)}{1 + (1 - 2X_s)(S_2 + \beta)}\right]\right\} \tag{3}$$

Substituting Eq 3 into Eq 2 produced (after much manipulation) Eq 4 as an alternative expression for the Δp_{cq}-ratio.

$$\frac{\Delta p_{cq}}{p_0} = \frac{2\beta(1 - X_s)}{(1 - S_2 - \beta)(1 + S_2)} \tag{4}$$

Equation 4 shows that the relative magnitude of the quasi-preconsolidation effect depends primarily on β and X_s. But Ref *1* also shows that β has an approximately constant value averaging about 0.185 for the clays tested. As explained previously, X_s depends on the relative strength increase mobilization along the Fig. 12*a* 2-3 ESP compared with the 2-4 ESP.

Substituting into Eq 4 then gives the quasi-preconsolidation effect predictions from this theory. Assuming ($K_0 = 1 - \sin \phi'$) gives [$S_2 = \sin \phi'/(2 - \sin \phi')$]. Assume that $\beta = 0.185$. We now come to the question of what sign (and magnitude) to use for X_s: +, −, or zero?—which the writer considers a fascinating question and one with almost no answer in the technical literature. The writer found only the experimental work of Newlin [*12*] in which he showed that $X_s = 0$ over about two log cycles of secondary compression time to 500 min, for three clays with PI from 5 to 16 percent and with the clays in undisturbed, remolded, and compacted conditions. For lack of any other data, assume that $X_s = 0$. Then Eq 4 predicts a quasi-preconsolidation effect of 48 percent for $\phi' = 15$ deg to 64 percent for $\phi' = 35$ deg. However, the author believes that more plastic clays and longer secondary aging times than investigated by Newlin [*12*] would show a positive $A_{2\text{-}3}$ and therefore a positive X_s. The quasi-preconsolidation decreases to 36 to 50 percent if $X_s = 0.25$ and to 24 to 32 percent if $X_s = 0.5$ (illustrated in Fig. 12*a*). These values all check approximately with the average of 40 percent (from laboratory data) suggested by Leonards and Alschaeffl [*11*].

One can also imagine circumstances where the present theory will predict a Δp_{cq}-effect less than the aforementioned 24 to 64 percent. If the fabric of the clay lacks the ability for the dispersion increase-in-d_ϵ behavior, then no strength increase will occur, S_4 will $= S_2$, $\beta = 0$, and Δp_{cq} will $= 0$. The writer has found no instance of such a lack and it seems unlikely for most clays. More likely, a clay might have such a sensitive fabric that it tends to collapse during secondary compression and causes the 2-3 ESP in Fig. 12*a* to go directly to the new virgin consolidation K_0-line. A_q and X_s would then both $= 1$, and Eqs 2 and 4 then predict $\Delta p_{cq} = 0$. The Ottawa clay described by Crawford and Burn [*13*] probably behaves with $A_q \simeq 1$.

The author has now proposed a physical phenomenon to explain the shear strength increase associated with aging, and shown quantitatively how this applies to produce the quasi-preconsolidation effect. This effect depends on the fabric-dispersion increase-in-d_ϵ behavior together with a sufficiently insensitive fabric to produce low A_q and X_s values.

Other Practical Aspects of Dispersion-d_ϵ Behavior

Dynamic Modulus Correction

As noted in the section on Increasing Time for Secondary Compression, engineers have discovered that they must increase the dynamic values of E and G determined from undisturbed samples and laboratory reconsolidation of the clay in order to match *in situ* data. Anderson and Woods [*9*] note typical correction factors of about 1.5 to 3.5, depending on the relative secondary compression ages of the laboratory and *in situ* clay. The need for the correction probably results from the *in situ* clay having experienced a much longer secondary aging than the reconsolidated laboratory samples, giving more time for the time-dispersion-d_ϵ transfer and thus producing a stiffer fabric in the *in situ* clay.

Need to Age Laboratory Samples

The aforementioned modulus correction also suggests the need for a possible aging correction to laboratory shear strength data, or the appropriate aging of laboratory test samples, or a combination. The same longer *in situ* secondary times can increase the ordinary quasi-static shear test moduli (see Fig. 9) and strengths. It seems clear that laboratory samples will better duplicate *in situ* behavior if the clay in the samples better duplicates the fabric of the clay *in situ*. For some clays, and perhaps most clays, producing an adequately similar fabric in the laboratory samples would require long aging times at constant stress under drained conditions. Engineers do not commonly do this at present, but perhaps they should move in this direction.

Need for Stress-Rest Control Testing

The application of loads on cohesive soils in the field often involves a slow rate with interspersed periods of rest. Such application should allow time for a possibly significant dispersion-d_ϵ clay fabric stress transfer to occur, with the consequent reduced clay compressibility and increased strength. When

modeling a loading sequence in the laboratory, say by the stress path simulation method, the engineer should for best results also allow the appropriate changes in fabric to occur in the laboratory sample. This requires stress-controlled testing, with appropriate rest stops at constant stress. Such testing can perhaps duplicate in the sample the clay fabric changes that would occur *in situ*. The research outlined in this paper has shown that testing with ordinary constant strain rates does not allow the dispersion-d_ϵ transfer and strengthening phenomenon to occur, or at least to occur fully. Because this transfer has a potentially important effect, engineers should sometimes consider giving up the convenience of strain-control testing and go back to the "old fashioned" stress control methods.

Aging Strength Not Due to Clay Bonding

Many engineers have assumed, and some have attempted to prove, that the clay strength increases from constant-stress aging in the laboratory result from increased bond formation between the clay particles. This probably occurs over geologic time intervals, as when clay turns to claystone and shale. However, the research outlined in this paper leads to the opposite conclusion that these strength increases have nothing to do with bond formation over the range of typical laboratory aging times.

Figure 1 shows that the I_0-intercept, which equals that shear resistance not dependent on effective stress and therefore due to internal bonding, forms a part of the larger I-component. Any increase in I_0 should usually show as an increase in I, but the I-component stayed remarkably constant during the various clay treatments that increased the total clay shear strength. The D-component always increased to account for the total strength increase. It seems clear from these results that the I_0 bond strength did not increase measurably with laboratory aging and that d_ϵ increased greatly. The realization that the d_ϵ-component increase produces the strength increases during laboratory aging led the author to consider how this could happen, which in turn led to the hypothesis given in the section on Hypothesis for Dispersion-d_ϵ Behavior.

A more general recognition that aging over laboratory aging times, and probably also over engineering project life spans, involves a fabric dispersion and stress transfer adjustment rather than a bonding phenomenon should save some further false starts and help the profession to more quickly reach a better understanding of clay particle mechanics and clay fabric and structure, and particularly how these change with engineering time.

Conclusions

1. A variety of laboratory experimental studies, which involved special shear strength component testing in several clays that had undergone various chemical, stress, and time treatments, all resulted in an increase in the frictional component of shear resistance with no measurable change in the bond component.

2. This paper suggests a clay fabric modification process to explain the friction increase behavior. This process involves a pervasive, continuing fabric dispersion with an associated transfer of shear load to stiffer and stronger particle aggregates within the fabric.

3. A better recognition of the dispersion-friction process may produce some important practical results. Among these the author quantitatively describes the quasi-preconsolidation effect and notes how to best duplicate or otherwise take advantage of the clay "aging" effects that can both increase subsequent shear modulus and reduce compressibility.

Acknowledgments

Dr. Frank Townsend, Professor of Civil Engineering at the University of Florida, kindly reviewed several drafts of this paper and made important suggestions.

References

[1] Schmertmann, J. H. in *Laurits Bjerrum Memorial Volume*. Norwegian Geotechnical Institute, Oslo, 1976, pp. 65–98.

[2] Schmertmann, J. H. and Osterberg, J. O. in *Proceedings*, Research Conference on Shear Strength of Cohesive Soils, American Society of Civil Engineers [hereafter cited as ASCE], Boulder, Colo., 1961, pp. 643–694.

[3] Schmertmann, J. H., "An Experimental Study of the Development of Cohesion and Friction with Axial Strain in Saturated Cohesive Soils," Ph.D. dissertation, Northwestern University, Evanston, Ill., June 1962.

[4] Schmertmann, J. H., *Journal of the Soil Mechanics and Foundations Division*, ASCE, Vol. 88, No. SM6, 1962, pp. 169–205.

[5] Lambe, T. W., *The Structure of Organic Soil*, ASCE, *Proceedings*, Vol. 79, Separate No. 315, 1953.

[6] Schmertmann, J. H. and Hall, J. R., Jr., in *Transactions*, ASCE, Vol. 128, Part I, 1961, pp. 949–981; also published in *Journal of the Soil Mechanics and Foundations Division*, ASCE, Proceedings Paper 2881, Aug. 1961.

[7] Schmertmann, J. H. and Hall, J. R., Jr., *Journal of the Soil Mechanics and Foundations Division*, ASCE, Vol. 88, No. SM4, 1962, pp. 163–167; also in Ref 6, pp. 976–981.

[8] Schmertmann, J. H., *Journal of the Soil Mechanics and Foundations Division*, ASCE, Vol. 91, No. SM2, Part 1, 1965, pp. 131–315.

[9] Anderson, D. G. and Woods, R. D., *Journal of the Geotechnical Engineering Division*, ASCE, Vol. 102, No. GT5, May 1976, pp. 525–537.

[10] Bea, R. G., *Journal of the Soil Mechanics and Foundations Division*, ASCE, Vol. 89, No. SM1, 1963, pp. 268–277.

[11] Leonards, G. A. and Altschaeffl, M., *Journal of the Soil Mechanics and Foundations Division*, ASCE, Vol. 90, No. SM5, Sept. 1964, p. 148.

[12] Newlin, C. W., "A Laboratory Investigation of Lateral Stresses during One-Dimensional Consolidation," Ph.D. dissertation, Northwestern University, Evanston, Ill., June 1965.

[13] Crawford, C. B. and Burn, K. N. in *Laurits Bjerrum Memorial Volume*, Norwegian Geotechnical Institute, Oslo, 1976, pp. 117–124.